scientific reports

Check for updates

OPEN

# Long COVID diagnostic with differentiation from chronic lyme disease using machine learning and cytokine hubs

Bruce K. Patterson[1]✉, Jose Guevara-Coto[1], Javier Mora[2], Edgar B. Francisco[1], Ram Yogendra[3], Rodrigo A. Mora-Rodríguez[2], Christopher Beaty[1], Gwyneth Lemaster[1], Gary Kaplan DO[4], Amiram Katz[5] & Joseph A. Bellanti[6]

**The absence of a long COVID (LC) or post-acute sequelae of COVID-19 (PASC) diagnostic has profound implications for research and potential therapeutics given the lack of specificity with symptom-based identification of LC and the overlap of symptoms with other chronic inflammatory conditions. Here, we report a machine-learning approach to LC/PASC diagnosis on 347 individuals using cytokine hubs that are also capable of differentiating LC from chronic lyme disease (CLD). We derived decision tree, random forest, and gradient-boosting machine (GBM) classifiers and compared their diagnostic capabilities on a dataset partitioned into training (178 individuals) and evaluation (45 individuals) sets. The GBM model generated 89% sensitivity and 96% specificity for LC with no evidence of overfitting. We tested the GBM on an additional random dataset (106 LC/PASC and 18 Lyme), resulting in high sensitivity (97%) and specificity (90%) for LC. We constructed a Lyme Index confirmatory algorithm to discriminate LC and CLD.**

**Keywords** COVID-19, PASC, Long COVID, Cytokines, Chronic lyme disease (CLD), Myalgic encephalomyelitis-chronic fatigue syndrome (ME-CFS), Machine Learning/AI

LC or PASC is a clinical unmet need affecting around 20–30 million Americans and many more worldwide. A non-subjective diagnosis for LC/PASC has remained elusive even after multiple reports of symptoms for LC. Symptom-based classification of immunologic diseases including autoimmune diseases and chronic inflammatory diseases can be difficult because of non-specific or overlapping symptoms[1]. A recent report suggested the use of cytokine hubs to more precisely categorize autoimmune diseases with the stated oal of using the information as therapeutic targets as the expansion of immune-based therapy grows[1]. The heterogeneity of immune-mediated inflammatory diseases (IMIDS) described in this publication also applies to post-infectious immune-mediated and inflammatory conditions currently in the discussion of LC/PASC.

The symptoms of LC/PASC have been well described in the literature[2–4] and a recent article[2] concluded that fatigue, post-exertional malaise, and brain fog were diagnostic of LC. This conclusion, however, identified symptom presentations of LC/PASC that overlap significantly with chronic lyme disease (CLD), myalgic encephalomyelitis/chronic fatigue syndrome (ME/CFS), and other post-infectious chronic inflammatory disorders[5–7]. Clear etiological and pathophysiological differences exist in these chronic inflammatory conditions that necessitate precision medicine-tailored therapies.

We previously used machine learning to distinguish long COVID from active COVID-19 infections using immune/inflammatory biomarkers[2]. Similarly, there are multiple articles on machine learning in acute COVID-19 that focus on forecasting of disease and mortality[8,9] or on the analysis of CXR or images[10–12]. Here, we present a very different machine learning/cytokine hub approach to diagnose LC/PASC and differentiate LC/PASC from CLD using immune/inflammatory biomarkers in plasma.

[1]IncellDx Inc, 30920 Huntwood Ave, San Carlos, Hayward, CA 94544, USA. [2]Lab of Tumor Chemosensitivity, Faculty of Microbiology, CIET/CICICA, Universidad de Costa Rica, San José, Costa Rica. [3]Lawrence General Hospital, Lawrence, MA, USA. [4]Department of Community and Family Medicine, Georgetown University School of Medicine, Washington, DC, USA. [5]Neurology Specialist Affiliated With Norwalk Hospital, Orange, CT, USA. [6]Departments of Pediatrics and Microbiology-Immunology, and the International Center for Interdisciplinary Studies of Immunology, Georgetown University Medical Center, Washington, DC, USA. ✉email: brucep@incelldx.com

# Methods

## Patients

The Chronic Covid Treatment Center Institutional Review Board reviewed and approved the protocol. All participants provided written informed consent to participate in the research. The date of acute COVID-19 infection was defined as the date of the first positive SARS-CoV-2 test result or COVID-19 symptom onset. Healthy control participants had no known history of SARS-CoV-2 infection and a negative anti-NP assay at the time of participation. All methods were performed in accordance with the relevant guidelines and regulations as set forth by the review board. All patients were over 18 years old.

Mild Acute COVID-19:

1. Fever, cough, sore throat, malaise, headache, myalgia, nausea, diarrhea, loss of taste and smell,
2. No sign of pneumonia on chest imaging (CXR or CT Chest),
3. No shortness of breath or dyspnea.

Moderate Acute COVID-19:

1. Radiological findings of pneumonia fever and respiratory symptoms,
2. Saturation of oxygen (SpO2) ≥ 94% on room air at sea level.

## LC/PASC

Inclusion criteria for individuals in the LC group were previous confirmed or probable COVID-19 infection (according to World Health Organization guidelines) age ≥ 18 years; and persistent symptoms > 12 weeks after initial COVID-19 infection. Symptoms included those previously described and scored[4].

Inclusion criteria for healthy controls (HC) were age ≥ 18 years, no previous SARS-CoV-2 infection and a negative history taken as part of registration in the Chronic COVID Treatment Center (CCTC).

## Chronic lyme disease (CLD)

Patients presented to the CCTC with a history of fatigue, brain fog, and post-exertional malaise that pre-dated the SARS-CoV-2 pandemic (pre-2020) and persisted for greater than 6 months (as per the ILADS Working Group)[13].

Presence of *Borrelia Burgdorferi sp* were confirmed by 2-tiered immunologic testing which includes immunoblot testing. Presence of other tick-borne organisms was noted but not required for definition of CLD as previously described[13].

## Multiplex cytokine/chemokine profiling

Plasma collected in plasma preparation tubes (PPT, BD Biosciences, San Jose CA) as used for cytokine quantification using acustomized 14-plex bead based flow cytometric assay (IncellKINE, IncellDx, Inc) on a CytoFlex flow cytometer as previously described using the following analytes: TNF-a, IL-4, IL-13, IL-2, GM-CSF, sCD40L, CCL5 (RANTES), CCL3 (MIP-1a), IL-6, IL-10, IFN-g, VEGF, IL-8, and CCL4 (MIP-1b)[2]. For each patient sample, 25 µL of plasma was used in each well of a 96-well plate. Samples were analyzed on a Beckman Coulter CytoFlex LX 3-laser flow cytometer using Kaluza Analysis Software (Beckman-Coulter, Miami, FL). All statistical analysis was performed using the Mann–Whitney test and a P value ≤ 0.05 was considered statistically significant.

## Data acquisition and processing for machine learning model construction

To construct a working dataset we selected cytokine profiles from three disease states: Not Perturbed (NP), LC/PASC, and CLD. The Not Perturbed class represented the aggregation of unaffected (healthy controls) and mild- moderately affected COVID-19 individuals. We combined the categories based on the lack of chronic immunologic perturbation as previously published[4] and as present in chronic disease states like PASC and CLD. The absence of statistical difference between the two states when comparing the IncellKine cytokine profiles ($p$-value > 0.05) using a Mann–Whitney U-test further supports this classification. Severe COVID-19 individuals, corresponding to individuals affected by COVID-19 with severe manifestations and immunological perturbations, were excluded. Outliers were removed using an isolation forest (contamination parameter = 5%), generating a dataset consisting of 67 Not Perturbed, 103 PASC, and 53 CLD. Each individual had cytokine profiles derived from the incellKINE assay (14-plex cytokine panel), the LHI (long hauler index), and SI (severity index) calculated according to Eqs. (1) and (2), as reported in Ref.[2]:

$$LHI = \frac{IL-2+IFN-gamma}{CCL4} \tag{1}$$

$$SI = \frac{\left(IL-6+\frac{sCD40L}{1000}+\frac{VEGF}{10}+(10*IL-10)\right)}{(IL-2+IL-8)} \tag{2}$$

The dataset was then imported into Python using the Pandas library[14–16]. Data was partitioned with stratification using the train_test_split function from the model_selection module sci-kit-learn[17]. An 80% of the data was for training and a 20% hold-out evaluation split was used to obtain performance metrics and identify overfitting. Table 1 contains the number of instances in the pre-split dataset, training, and evaluation partition.

| Data partition \| Label | Not Perturbed | PASC | CLD |
|---|---|---|---|
| Full dataset | 67 | 103 | 53 |
| 80% training | 54 | 82 | 42 |
| 20% evaluation | 13 | 21 | 11 |

**Table 1.** The number of individuals for each disease state (class) in the full dataset, the training and evaluation partitions.

## Construction of tree-based machine learning classifiers: decision tree, random forest, and gradient boosting machine

In our study, we employed three tree-based machine learning classifiers: a decision tree, a random forest, and a gradient-boosting machine. The decision tree and random forest were implemented using the sci-kit-learn library, whereas the gradient-boosting machine utilized the LightGBM library. Hyperparameter optimization for each model involved a range of settings. For the decision tree, parameters like criterion, class weight, splitter, maximum depth, minimum samples split, and leaf were adjusted. The random forest model's parameters included the number of estimators, criterion, maximum depth, minimum samples split and leaf, and bootstrap options. For the gradient-boosting machine, we varied the learning rate, number of estimators, minimum data in leaf, and depth. Hyperparameter tuning was conducted using tenfold cross-validation with three repeats, selecting the best model based on the F1 score. Performance was assessed on a 20% hold-out evaluation split. A custom classification report, which included recall, specificity, precision, negative predictive value, and F1 score was used to calculate performance metrics and determine if there was model overfitting. The model demonstrating the highest performance was assigned to the best_model variable.

## Development of a lyme index for further differentiation of PASC and lyme

To confirm the differentiation of CLD and LC/PASC individuals following screening, and reduce classification errors, two new features were generated. These features were part of the Lyme Index. To develop these features we implemented an approach based on immunological significance and domain expertise. We generated the features through a programmatic method that implemented combinations of different operations on the features (ratios, powers, multiplication, and sums). This approach focused on placing important cytokines for CLD in the numerator and for LC/PASC in the denominator. The generated sets of features were filtered to remove potential zero-divisions and curated by domain experts to confirm their biological relevance.

To determine the Lyme Index's ability to classify CLD patients, we used a dataset comprised of 25 randomly-selected CLD individuals. A decision tree was trained using the 2 features and tested on the dataset. Because only one class was present (CLD), we only calculated sensitivity, PPV (precision), and accuracy.

## Prediction of patient disease state on blinded records using the best-performing model

To determine the predictive capability of the highest-performing model upon deployment, we enrolled 125 randomly selected individuals. Individuals were processed to identify clinical assessment data, confirming their disease state (NP, LC/PASC, or CLD). Individuals from the dataset were confirmed to belong to either LC/PASC or CLD disease states. Patients without clinical assessment data and/or a diagnosis different from the classes in the model were removed to properly calculate performance metrics. These criteria resulted in the removal of only one patient profile. The resulting dataset was composed of 124 individuals, 18 CLD, and 106 LC/PASC patients defined by the same criteria as the test set patients and according to the methods above for LC/PASC and CLD[4,13]. The independent datasets comprise a group of individuals with age, gender, and predominant symptoms as summarized in Table 2.

| Characteristic | LC/PASC n = 106 | CLD n = 18 |
|---|---|---|
| Age-year | | |
| Median | 45 | 41 |
| Range | 25–70 | 19–78 |
| Sex % | | |
| Male | 43 | 32 |
| Female | 57 | 68 |
| Symptoms % | Fatigue (100) | Fatigue (93) |
| | Brain Fog (98) | Brain Fog (50) |
| | PEM (83) | PEM (43) |
| | Headache (57) | Headache (14) |

**Table 2.** Demographics and Clinical Characteristics of LC/PASC and CLD Cohorts.

## Ethics

All the patients/participants provided their written informed consent to participate in this study. The study was approved by the IRB for the Chronic COVID Treatment Center.

## Results

### Cytokine parameters reveal no difference between healthy controls and mild-moderate acute COVID individuals, supporting aggregation into the not perturbed disease state

To determine the immunologic distinctions between healthy individuals (Control) and those with mild to moderate acute COVID-19 (MM), we evaluated the 14 cytokines, the LHI, and SI with a Mann-Whitey U-test. The outcome of our analysis (Table 3) revealed that only VEGF showed a statistically significant trend ($p = 0.09$) between the HC and MM groups. The remaining 15 biomarkers, including the LHI and SI, did not have statistical differences.

To elucidate the broader immune landscape, we aggregated metrics from both groups. The resultant *p*-value of 0.1883 underscores the absence of a statistically significant difference between the many chronic inflammatory biomarkers from healthy control (HC) and mild-moderate (MM) individuals. We aggregated the HC and MM based on this lack of statistically significant differences in these cytokines to demonstrate the diagnostic capability of the model in a population with ongoing acute COVID-19 cases.

### Tree-based models for diagnosis of PASC and differentiation from chronic lyme disease

To evaluate the predictive capability of the tree-based models (decision tree, random forest, and GBM), we used a hold-out partition from the dataset. This split was a stratified sample of 20% of the complete dataset. The resulting performance metrics were compared to those obtained from the training partition. This comparison allowed us to determine if the models presented overfitting. The similarity of metrics between the training set and hold-out set indicates that the model did not show overfitting and had proper predictive capabilities. Table 4 indicated that GBM had the overall best-weighted performance and the smallest training time. These two characteristics allowed us to select GBM as the best model for validation on a random sample.

To interpret the GBM model, we approximated its decision pathways using a surrogate decision model. This allowed us to visualize the more complex GBM into a simplified single-tree topology. Figure 1 represents the binary decision path used by the GBM to classify between Not Perturbed, LC/PASC, and CLD. The tree shows

| Biomarker | Mean (HC) | Median (HC) | Std (HC) | Mean (MM) | Median (MM) | Std (MM) | U-test p-value | Significance |
|---|---|---|---|---|---|---|---|---|
| TNF-α | 9.29 | 8.41 | 4.97 | 7.15 | 6.02 | 3.73 | 0.05 | ns |
| IL-4 | 7.29 | 3.58 | 10 | 2.55 | 1.56 | 2.31 | 0.19 | ns |
| IL-13 | 3.69 | 2.15 | 5.11 | 2.41 | 1.02 | 4.01 | 0.15 | ns |
| IL-2 | 8.64 | 9.47 | 3.84 | 10.24 | 9.54 | 2.26 | 0.15 | ns |
| GM-CSF | 36.83 | 10.96 | 61.42 | 53.85 | 10.08 | 100.8 | 0.25 | ns |
| sCD40L | 12,163.45 | 7966.35 | 14,245.54 | 11,121.09 | 7383.9 | 9720.52 | 0.57 | ns |
| CCL5 | 11,776.36 | 11,105.19 | 5666.6 | 11,781.82 | 11,204.37 | 3387.49 | 0.28 | ns |
| IL-6 | 3.15 | 2.51 | 2.53 | 9.42 | 2.28 | 21.59 | 0.22 | ns |
| IL-10 | 1.41 | 1.06 | 0.97 | 1.17 | 0.96 | 0.65 | 0.17 | ns |
| IFN-γ | 3.37 | 1.41 | 4.13 | 1.02 | 0.73 | 0.93 | 0.1 | ns |
| IL-8 | 14.12 | 9.64 | 19.47 | 10.84 | 9.97 | 5.65 | 0.61 | ns |
| CCL4 | 12.86 | 10.55 | 7.14 | 14.44 | 10.84 | 11.59 | 0.43 | ns |
| LHI | 1.16 | 1.14 | 0.64 | 1.1 | 1.12 | 0.54 | 0.16 | ns |
| SI | 3.42 | 1.18 | 6.84 | 1.78 | 1.32 | 1.9 | 0.11 | ns |

**Table 3.** Statistical comparison between HC and MM using a Mann–Whitney U-test. For p-values greater than 0.05, ns represent a lack of statistically significant difference.

| Train/Test | Model | Sensitivity | Specificity | F1 | PPV | NPV | Accuracy | Training/Tuning Time (seconds) |
|---|---|---|---|---|---|---|---|---|
| Train | DT | 97 | 99 | 0.97 | 98 | 97 | 97 | 0.06 |
| Train | RF | 100 | 100 | 1 | 100 | 100 | 100 | 2.26 |
| Train | GBM | 100 | 100 | 1 | 100 | 100 | 100 | 0.86 |
| Test | DT | 84 | 94 | 0.84 | 84 | 94 | 84 | Not measured |
| Test | RF | 89 | 95 | 0.89 | 89 | 95 | 89 | Not measured |
| Test | GBM | 89 | 96 | 0.89 | 89 | 96 | 89 | Not measured |

**Table 4.** Weighted LC diagnostic performance metrics (in percentages) on the training (80%) and hold-out (20%) partitions for the three tree-based models: decision tree (DT), random forest (RF), and gradient boosting machine (GBM).

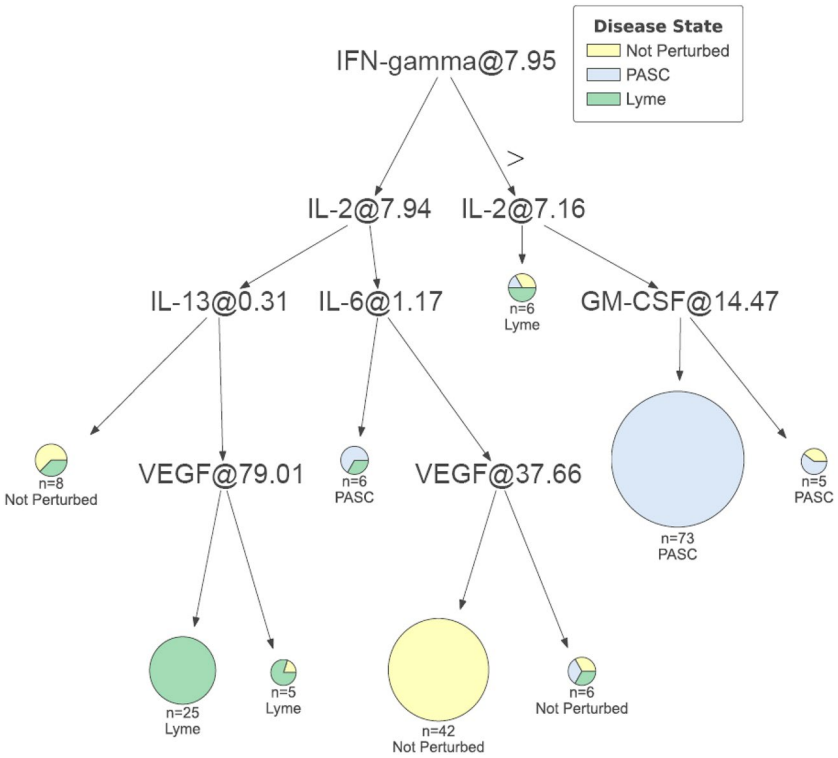


**Fig. 1.** Surrogate tree visualization of the GBM classifier's decision paths. Nodes branching left are indicative of less than or equal (≤) values, while nodes branching right represent greater than (>) values.

high levels of IL-2 lead to LC/PASC, whereas lower levels of the IL-2 are associated with chronic CLD and Not Perturbed individuals. We also determined that altered levels of VEGF are associated with chronic CLD similar to Antonara et al.[18].

## Validation of the LightGBM model on a random set

To corroborate the robustness of the GBM model, we evaluated its predictive capabilities on an independent and randomly selected dataset composed of 124 patients (18 CLD and 106 LC/PASC) presenting with fatigue. The result (Table 5) indicated a weighted Sensitivity of 99% and Specificity of 88% for the detection of LC/PASC, and weighted Sensitivity of 89%, and a Specificity of 99% for CLD. The GBM model demonstrated its ability to discern between diverse disease states with high-performance metrics. The use of an external dataset validates the results in the 20% holdout split and supports the potential deployment of this model as a clinical diagnostic. This classification algorithm demonstrates the ability to distinguish not perturbed (includes acute COVID) from LC/PASC and CLD. The high positive (PPV) and negative predictive values (NPV) in Table 5 not only demonstrate the ability of the algorithm to show who does have CLD or LC/PSC (PPV) but also demonstrates the abilty to show who does not have either of these two chronic inflammatory conditions.

## Development of the CLD index

To reduce the presence of misclassified instances (especially false negatives) and to confirm the GBM model if patients are not in the non-perturbed screening category, we developed a heuristic capable of further discriminating between LC and CLD. We used a domain expert-based approach to engineer a novel two-feature biomarker (Eqs. 3 and 4) known as CLD Index. The need for a two-dimensional feature space was due to the complexity of separating. Implementation of the CLD Index allowed for improved separation as they represented

| Class\|Metric | Sensitivity (%) | Specificity (%) | PPV (%) | NPV (%) | F1 | Accuracy |
|---|---|---|---|---|---|---|
| PASC | 99.06 | 88.89 | 98.13 | 94.12 | 0.986 | |
| CLD | 88.89 | 99.06 | 94.12 | 98.13 | 0.914 | |
| Weighted | 97.58 | 90.36 | 97.55 | 94.70 | 0.950 | 94% |

**Table 5.** Performance metrics of the GBM model on a random set of patients to validate deployment potential.

the biological relationships of cytokines and disease states, with CLD-elevated cytokines (TNF-alpha and IL-4) in the numerator and PASC-elevated cytokines (IFN-gamma, IL-2 and CCL3) in the denominator.

$$Lyme\ Index\ Feature\ 1 = \frac{(TNF - alpha + IL - 4)}{(IFN - gamma + IL - 2)} \tag{3}$$

$$Lyme\ Index\ Feature\ 2 = \frac{(TNF - alpha * IL - 4)}{(IFN - gamma + IL - 2 + CCL3)} \tag{4}$$

The discriminating power of features 1 and 2 was evaluated using a decision tree and a holdout partition of 20%. Further evaluation was done on a a 25-CLD patient dataset. The results indicated a high discriminating power, with 100% sensitivity and specificity when evaluating the holdout set (Table 6). This effectiveness was confirmed when testing features 1 (TNF-alpha + IL-4)/(IFN-gamma + IL-2) and 2 (TNF-alpha * IL-4)/(IFN-gamma + IL-2 + CCL3) on the 25-CLD dataset, where sensitivity, accuracy, and PPV were 100%. The power of the CLD Index can be attributed to engineering a set of features where relevant CLD cytokines are in the numerator and relevant LC/PASC cytokines are in the dominant. This leads to higher CLD Index values for CLD patients and lower values for PASC individuals.

## Discussion

Acute COVID causes a constellation of immunologic abnormalities characterized as a "Cytokine Storm". Frequently lost in this pathology is significant immunosuppression due to low T-cell count, especially CD8 + T-cells, immune exhaustion, and decreased expression of Granzyme A[19–22]. Immunosuppression can lead to the reactivation of chronic herpes family viruses such as Epstein-Barr virus (EBV), cytomegalovirus (CMV), Human Herpesvirus-6 (HHV-6), and Herpes Simplex (HSV) among others. In addition, undiagnosed or inadequately treated tick-borne illnesses such as CLD may also recrudesce because of a diminution of immune control. Diagnosis and differentiation of all of these "sequelae" of acute COVID are difficult when SARS-CoV-2 itself can produce a post-infectious condition (LC/PASC) and the symptoms significantly overlap.

Cytokine profiling provides valuable information for the understanding of the complex immunological interactions regulating the mechanisms and outcomes of different pathologies. Combining the obtained data with machine learning approaches has been successfully used for the prediction of severity, chronicity, and mortality rate of diseases such as COVID-19[2,23]. Translation of these integrated analyses into diagnostic tools represents a promising strategy to facilitate the differential diagnosis of pathologies with unspecific and similar clinical manifestations driven by distinct immunopathological mechanisms.

Immune-mediated inflammatory diseases such as LC/PASC and CLD share a common spectrum of symptoms including pain, fatigue, depression, and cognitive deficits[2,24]. Therefore, it is important to identify specific immunological features among these diseases to improve the current diagnostic tools available and provide adequate treatment to the patients.

To address the need for accurate diagnosis for proper treatment, we developed the Lyme Index, a diagnostic score, to improve the stratification of LC/PASC and CLD patients. The Lyme Index uses two engineered features, derived from biologically relevant cytokines, where CLD cytokines are in the numerator and LC/PASC cytokines are in the denominator creating a ratio where higher scores were associated with CLD, the lower scores were LC/PASC. As we previously described, LC/PASC patients are characterized by increased levels of IFN-γ and IL-2, which in the context of a viral infection would induce the activation of effector T cells with pro-inflammatory properties. However, the chemotactic milieu in these patients, characterized by lower CCL4 and higher CCL3, induces the attraction mainly of myeloid cells promoting the inflammatory response associated with the long-lasting symptoms observed in LC/PASC. Additionally, increased IFN-γ promotes myeloid cell activation that, as we have previously characterized, is associated with the increased frequency of inflammatory CD14 +, CD16 +, and CCR5 + monocytes in the PASC group compared to healthy donors[2,25], supporting lymphopenia and virus persistence. Our diagnostic index integrates the increased levels of IFN-γ, IL-2, and CCL3 in LC/PASC patients to separate them from clinically similar chronic CLD patients.

In the case of CLD patients, we observed an increased concentration of TNF-α and IL-4 and included these parameters in our index to further stratify these patients. Augmented levels of these cytokines were previously reported in the cerebrospinal fluid of patients with neuroborreliosis compared with control

| Metric\|Features | (TNF-alpha + IL-4)/(IFN-gamma + IL-2) and (TNF-alpha * IL-4)/(IFN-gamma + IL-2 + CCL3) (%) |
|---|---|
| Sensitivity 80/20 evaluation split | 100 |
| Specificity 80/20 evaluation split | 100 |
| Precision 25-CLD | 100 |
| Recall 25-CLD | 100 |
| Accuracy 25-CLD | 100 |
| F1-Score 25-CLD | 100 |

**Table 6.** Performance metrics for the CLD Index (features 1 and 2) on the evaluation partition and the 25-CLD dataset.

subjects [26]. Additionally, in a different study, an increase in IL-4 concentration in cerebrospinal fluid of patients with neuroborreliosis was observed during the first months after the onset of neurological symptoms, followed by an increased IL-4 in blood at later time points[27], indicating that higher blood levels of IL-4 reflect an immunological alteration initiated in the central nervous system. As mentioned above, CLD patients are affected with persistent symptoms such as musculoskeletal pain, fatigue, and neurocognitive difficulties[24]. The mechanisms underlying the pathogenesis of the CLD syndrome are still not fully elucidated. Current evidence supports the hypothesis of an association with autoimmune events resulting in a dysregulated pro-inflammatory reaction, as well as, a chronic inflammation caused due to a slow clearance of the bacterial peptidoglycan[5,28]. Considering the type of symptoms observed in CLD that share the common features of exacerbated central nervous system pain and sensory-processing mechanisms, CLD is included within the group of pathologies associated with central sensitivity syndrome (CSS)[24]. Pro-inflammatory cytokines such as TNF-α promote CSS inducing central sensitization and hyperalgesia via distinct and overlapping synaptic mechanisms in neurons either by increasing excitatory synaptic transmission or by decreasing inhibitory synaptic transmission[29]. Furthermore, TNF-α promotes CSS-associated neuroinflammation generating several adverse effects, such as chronic pain, neurodegeneration, and cognitive impairment[30], common features of CLD. Additionally, immune cells promote peripheral or central nervous system sensitization through pro-inflammatory molecules such as TNF-α. Mast cells and astrocytes release TNF-α affecting neuronal function and promoting the development of chronic pain[30,31]. The effects of chronic inflammation and TNF-α, in particular, have been shown to lower levels of serotonin leading to depression[32]. Interestingly, a recent paper has suggested that low serotonin in LC could be alleviated by the use of Prozac™[33]. One can also speculate that effective treatment of chronic inflammation in LC and CLD might also be effective in addressing depression in these conditions.

Interestingly, CLD patients show elevated levels of IL-4, a cytokine associated with type 2 responses. Exacerbation of type 2 inflammation could be detrimental in different organs including the central nervous system. In an experimental model of neuromyelitis optica, a strong type 2 response in the central nervous system is observed promoting tissue damage in this pathology[34]. However, there is no direct association between type 2 responses and CLD or CSS. Considering the above-mentioned effects of pro-inflammatory cytokines such as TNF-α, the increased IL-4 production might be related to a compensatory mechanism to ameliorate the immune-mediated effects observed in CLD. Pro-inflammatory cytokines associated with neuroinflammation can feedback control their expression and regulate the production of other mediators like IL-4[35]. Further, TNF-α signaling induces the expression of GATA-3[36], which is the transcription factor associated with Th2 polarization and IL-4 production, indicating that TNF-α is responsible not only for the inflammatory effects promoting CSS and the symptoms associated with chronic CLD disease but also for the observed increase in IL-4 production as a compensatory mechanism. IL-4 polarized M2 macrophages induce a sustained production of opioid peptides ameliorating pain and promoting pain resolution[37]. Additionally, T cells in the meninges secrete IL-4 to trigger the production of brain-derived neurotrophic factors to support neurogenesis in response to inflammatory-associated damage[38]. Thus, the high levels of TNF-α and IL-4 detected in CLD are closely associated with the clinical manifestations of this disease, with the induction of the immune-mediated damage, and with a failed compensatory response.

Even though increased TNF-α and IL-4 are very characteristic of CLD, a study comparing neuroborreliosis patients with control subjects showed a significant difference in the concentration of these cytokines. However, there was no difference in neuroborreliosis patients compared with tick-borne encephalitis or multiple sclerosis patients[26]. These data highlight the importance of considering the LC/PASC-associated cytokines in our index to generate a more solid platform for patient stratification.

Targeting individual cytokines underlying the immunopathogenesis of these conditions may provide a powerful new tool in the treatment of these immunologically mediated disorders using precision medicine. Further study may elucidate how pathogen or antigen persistence or reactivation could contribute to these classifications.

## Data availability

All requests for materials and raw data should be addressed to the corresponding author.

Received: 9 March 2024; Accepted: 22 August 2024
Published online: 26 August 2024

## References

1. Schett, G., McInnes, I. B. & Neurath, M. F. Reframing immune-mediated inflammatory diseases through signature cytokine hubs. *N. Engl. J. Med.* **385**, 628–639 (2021).
2. Patterson, B. K. et al. Immune-based prediction of COVID-19 severity and chronicity decoded using machine learning. *Front. Immunol.* **12**, 700782. https://doi.org/10.3389/fimm.u (2021).
3. Davis, H. E. et al. Characterizing LC in an international cohort: 7 months of symptoms and their impact. *EClinicalMedicine* **38**, 101019. https://doi.org/10.1016/j.eclinm (2021).
4. Thaweethai, T. et al. Development of a definition of postacute sequelae of SARS-CoV-2 infection. *JAMA* **329**, 1934–1946. https://doi.org/10.1001/jama.2023.8823 (2023).
5. Wong, K. H., Shapiro, E. D. & Soffer, G. K. A review of post-treatment CLD disease syndrome and chronic CLD disease for the practicing immunologist. *Clin. Rev. Allergy Immunol.* **62**, 264–271. https://doi.org/10.1007/s12016-021-08906-w (2022).
6. Bateman, L. et al. Myalgic encephalomyelitis/chronic fatigue syndrome: Essentials of diagnosis and management. *Mayo Clin. Proc.* **96**, 2861–2878. https://doi.org/10.1016/j.mayocp.2021.07.004 (2021).
7. Branda, J. A. & Steere, A. C. Laboratory diagnosis of CLD Borreliosis. *Clin. Microbiol. Rev.* **34**, e00018-19. https://doi.org/10.1128/CMR.00018-19 (2021).
8. Gao, Y. et al. Machine learning based early warning system enables accurate mortality risk prediction for COVID-19. *Nat. Commun.* **11**, 5033. https://doi.org/10.1038/s41467-020-18684-2 (2020).

9. Bousquet, A. et al. Deep learning forecasting using time-varying parameters of the SIRD model for COVID-19. *Sci. Rep.* **12**, 3030. https://doi.org/10.1038/s41598-022-06992-0 (2022).
10. Miyazaki, A. et al. Computer-aided diagnosis of chest X-ray for COVID-19 diagnosis in external validation study by radiologists with and without deep learning system. *Sci. Rep.* **13**, 17533. https://doi.org/10.1038/s41598-023-44818-9 (2023).
11. Wang, L., Lin, Z. Q. & Wong, A. COVID-Net: a tailored deep convolutional neural network design for detection of COVID-19 cases from chest X-ray images. *Sci. Rep.* **10**, 19549. https://doi.org/10.1038/s41598-020-76550-z (2020).
12. Nishio, M. et al. Deep learning model for the automatic classification of COVID-19 pneumonia, non-COVID-19 pneumonia, and the healthy: A multi-center retrospective study. *Sci. Rep.* **12**, 8214. https://doi.org/10.1038/s41598-022-11990-3 (2022).
13. Shor, S. et al. CLD Disease: An evidence-based definition by the ILADS Working Group. *Antibiotics* **8**, 269. https://doi.org/10.3390/antibiotics80402691 (2019).
14. Mckinney W. Pandas: a Foundational Python Library for Data Analysis and Statistics. http://pandas.sf.net [Accessed April 17, 2021]
15. Van Rossum G. Python programming language. in *USENIX annual technical conference*, 1–36.
16. Srinath KR. Python-The fastest growing programming language. *Int Res J Eng Technol* (2017) www.irjet.net [Accessed June 15, 2023].
17. Kramer, O. Scikit-learn. *Stud. Big Data* **20**, 45–53. https://doi.org/10.1007/978-3-319-33383-05 (2016).
18. Antonara, S., Ristow, L., McCarthy, J. & Coburn, J. Effect of Borrelia burgdorferi OspC at the site of inoculation in mouse skin. *Infect. Immun.* **78**, 4723. https://doi.org/10.1128/IAI.00464-10 (2010).
19. Rha, M. S. & Shin, E. C. Activation or exhaustion of CD8+ T cells in patients with COVID-19. *Cell. Mol. Immunol.* **18**, 2325–2333. https://doi.org/10.1038/s41423-021-00750-4 (2021).
20. Patterson, B. K. et al. CCR5 inhibition in critical COVID-19 patients decreases inflammatory cytokines, increases CD8 T-cells, and decreases SARS-CoV2 RNA in plasma by day 14. *Int. J. Infect. Dis.* **103**, 25–32. https://doi.org/10.1016/j.ijid.2020.10.101 (2021).
21. Song, J. W. et al. Immunological and inflammatory profiles in mild and severe cases of COVID-19. *Nat. Commun.* **8**, 3410. https://doi.org/10.1038/s41467-020-17240-2 (2020).
22. Turner, J. S. et al. SARS-CoV-2 Viral RNA shedding for more than 87 days in an individual with an impaired CD8+ T cell response. *Front. Immunol.* **8**, 618402. https://doi.org/10.3389/fimmu.2020.618402 (2021).
23. Castro-Castro, A. C. et al. Difference in mortality rates in hospitalized COVID-19 patients identified by cytokine profile clustering using a machine learning approach: An outcome prediction alternative. *Front. Med.* **9**, 987182. https://doi.org/10.3389/fmed.2022.987182 (2022).
24. Batheja, S., Nields, J. A., Landa, A. & Fallon, B. A. Post-treatment CLD syndrome and central sensitization. *J. Neuropsychiatry Clin. Neurosci.* **25**, 176–186. https://doi.org/10.1176/appi.neuropsych.12090223 (2013).
25. Patterson, B. K. et al. Persistence of SARS-CoV2-2 S1 protein in CD16+ monocytes in post-acute sequelae of COVID-19 (PASC) up to 15 months post-infection. *Front. Immunol.* **12**, 746021. https://doi.org/10.3389/fimmu.2021.746021 (2022).
26. Pietikäinen, A. et al. Cerebrospinal fluid cytokines in CLD neuroborreliosis. *J. Neuroinflamm.* **18**, 273. https://doi.org/10.1186/s12974-016-0745-x (2016).
27. Widhe, M. et al. Borrelia-specific interferon-gamma and interleukin-4 secretion in cerebrospinal fluid and blood during CLD borreliosis in humans: Association with clinical outcome. *J. Infect. Dis.* **189**, 1881–1891. https://doi.org/10.1086/382893 (2004).
28. Jutras, B. L. et al. *Borrelia burgdorferi* peptidoglycan is a persistent antigen in patients with CLD arthritis. *Proc. Natl. Acad. Sci. U. S. A.* **116**, 13498–13507. https://doi.org/10.1073/pnas.1904170116 (2019).
29. Kawasaki, Y., Zhang, L., Cheng, J. K. & Ji, R. R. Cytokine mechanisms of central sensitization: distinct and overlapping role of interleukin-1beta, interleukin-6, and tumor necrosis factor-alpha in regulating synaptic and neuronal activity in the superficial spinal cord. *J. Neurosci.* **28**, 5189–5194. https://doi.org/10.1523/JNEUROSCI.3338-07.2008 (2008).
30. Yang, J. X. et al. Potential neuroimmune interaction in chronic pain: A review on immune cells in peripheral and central sensitization. *Front. Pain Res.* **3**, 946846. https://doi.org/10.3389/fpain.2022.946846 (2022).
31. Li, T., Chen, X., Zhang, C., Zhang, Y. & Yao, W. An update on reactive astrocytes in chronic pain. *J. Neuroinflamm.* **16**, 140. https://doi.org/10.1186/s12974-019-1524-2 (2019).
32. Zhu, C. B., Blakely, R. D. & Hewlett, W. A. The proinflammatory cytokines interleukin-1beta and tumor necrosis factor-alpha activate serotonin transporters. *Neuropsychopharmacology* **10**, 2121–2131. https://doi.org/10.1038/sj.npp.1301029 (2006).
33. Wong, A. C. et al. Serotonin reduction in post-acute sequelae of viral infection. *Cell* **186**(4851–4867), e20. https://doi.org/10.1016/j.cell.2023.09.013 (2023).
34. Costanza, M. Type 2 Inflammatory responses in autoimmune demyelination of the central nervous system: Recent advances. *J. Immunol. Res.* **8**, 4204512. https://doi.org/10.1155/2019/4204512 (2019).
35. Vasudeva, K. et al. In vivo and systems biology studies implicate IL-18 as a central mediator in chronic pain. *J. Neuroimmunol.* **283**, 43–49. https://doi.org/10.1016/j.jneuroim.2015.04.012 (2015).
36. Santos, D. et al. TNF-alpha and Notch signaling regulates the expression of HOXB4 and GATA3 during early T lymphopoiesis. *In Vitro Cell. Dev. Biol. Anim.* **52**, 920–934. https://doi.org/10.1007/s11626-016-0055-8 (2016).
37. Celik, M. Ö., Labuz, D., Keye, J., Glauben, R. & Machelska, H. IL-4 induces M2 macrophages to produce sustained analgesia via opioids. *JCI Insight* **5**, e133093. https://doi.org/10.1172/jci.insight.133093 (2020).
38. Kipnis, J., Gadani, S. & Derecki, N. C. Pro-cognitive properties of T cells. *Nat. Rev. Immunol.* **12**, 663–669. https://doi.org/10.1038/nri3280 (2012).


## Author contributions

R.Y., J.G-C. organized the clinical study and actively recruited patients. B.K.P, C.B., J.G-C., E.B.F, performed experiments and analyzed the data. J.G., R.A.M., C.B., J.M. performed the statistics and bioinformatics B.K.P., J.G., E.B.F, J.M., R.Y. wrote and edited the draft of the manuscript and all authors contributed to revising the manuscript prior to submission.

## Competing interests

B.K.P, C.B., J.G, and E.B.F. are employees of IncellDx, Inc.

## Additional information

**Correspondence** and requests for materials should be addressed to B.K.P.

**Reprints and permissions information** is available at www.nature.com/reprints.

**Publisher's note** Springer Nature remains neutral with regard to jurisdictional claims in published maps and institutional affiliations.